

Contents lists available at ScienceDirect

Bone Reports

journal homepage: www.elsevier.com/locate/bonr

Case Report

A case of infantile osteopetrosis: The radioclinical features with literature update[☆]

Tamer Ahmed EL-Sobky^{a,*}, Ezzat Elsobky^b, Ismaiel Sadek^c, Solaf M. Elsayed^b, Mohamed Fawzy Khattab^d^a Department of Orthopaedic Surgery, Division of Paediatric Orthopaedics, Faculty of Medicine, Ain-Shams University, 38 Abbasia, Cairo, Egypt^b Division of Medical Genetics, Department of Paediatrics, Faculty of Medicine, Ain-Shams University, 38 Abbasia, Cairo, Egypt^c Department of Paediatrics, Faculty of Medicine, Ain-Shams University, 38 Abbasia, Cairo, Egypt^d Department of Orthopaedic Surgery, Faculty of Medicine, Ain-Shams University, 38 Abbasia, Cairo, Egypt

ARTICLE INFO

Article history:

Received 2 October 2015

Received in revised form 6 November 2015

Accepted 18 November 2015

Available online 19 November 2015

Keywords:

Malignant autosomal recessive

Skeletal imaging

Osteosclerosing dysplasia

Osteoclasts

ABSTRACT

Background: Osteopetrosis is a rare hereditary metabolic bone disorder characterized by generalized skeletal sclerosis caused by a defect in bone resorption and remodelling. Infantile autosomal recessive osteopetrosis is one of three subtypes of osteopetrosis and the most severe form. The correct and early diagnosis of infantile osteopetrosis is important for management of complications and for future genetic counselling. Diagnosis is largely based on clinical and radiographic evaluation, confirmed by gene testing where applicable.

Methods: Therefore, in this case study the classical clinical and radiological signs of a boy with infantile osteopetrosis will be presented with a comprehensive literature update. The differentiating signs from other causes of hereditary osteosclerosing dysplasias are discussed.

Results: This case study and review of available literature show that there tends to be a highly unique clinical and skeletal radiographic pattern of affection in infantile osteopetrosis.

Conclusion: Although tremendous advances have been made in the elucidation of the genetic defect of osteopetrosis over the past years, the role of accurate clinical and radiological assessment remains an important contributor to the diagnosis of infantile osteopetrosis.

© 2015 The Authors. Published by Elsevier Inc. This is an open access article under the CC BY-NC-ND license (<http://creativecommons.org/licenses/by-nc-nd/4.0/>).

1. Introduction

Osteopetrosis is a rare hereditary metabolic bone disorder characterized by generalized skeletal sclerosis caused by a defect in bone resorption and remodelling. The defect in bone turnover characteristically results in skeletal fragility despite increased bone mass, and it may also cause haematopoietic insufficiency. The actual incidence is unknown but it is estimated to be 1 case per 100,000–500,000 population (Stark and Savarirayan, 2009). Three distinct clinical forms of the disease—infantile, intermediate, and adult onset—are identified based on age and clinical features. Infantile autosomal recessive osteopetrosis is the more severe form that tends in the first few months of life. Hence, it is referred to as “infantile” and “malignant” compared to the autosomal dominant adult osteopetrosis (Stark and Savarirayan, 2009). The

correct and early diagnosis of infantile osteopetrosis (IO) is important for management of complications and for future genetic counselling. Diagnosis is largely based on clinical and radiographic evaluation, confirmed by gene testing where applicable (Sit et al., 2015). It is therefore important to be familiar with the radiological features of IO. Therefore, in this case study the classical clinical and radiological signs of a boy with infantile osteopetrosis will be presented and a comprehensive literature update. The differentiating signs from other causes of hereditary osteosclerosing dysplasias are discussed.

2. Case report

A one and a half year old boy was brought to our outpatient clinic with complaints of delayed milestones. He was first in order to a first cousin parents. Birth and family history were unremarkable.

Clinical examination revealed macrocephaly with opened anterior fontanel, frontal bossing, nystagmus of left eye and retromicrognathia, near normal stature and proportions and abnormal dentition. He had small chest cavity with ptosed liver and mildly enlarged spleen. The boy was only able to ambulate with parents' assistance.

[☆] The authors of the current study declare that no conflict of interest exists. No financing was received for research on which our study is based.

* Corresponding author.

E-mail addresses: tamersh@hotmail.com, tamer.ahmed@med.asu.edu.eg (T.A. EL-Sobky).

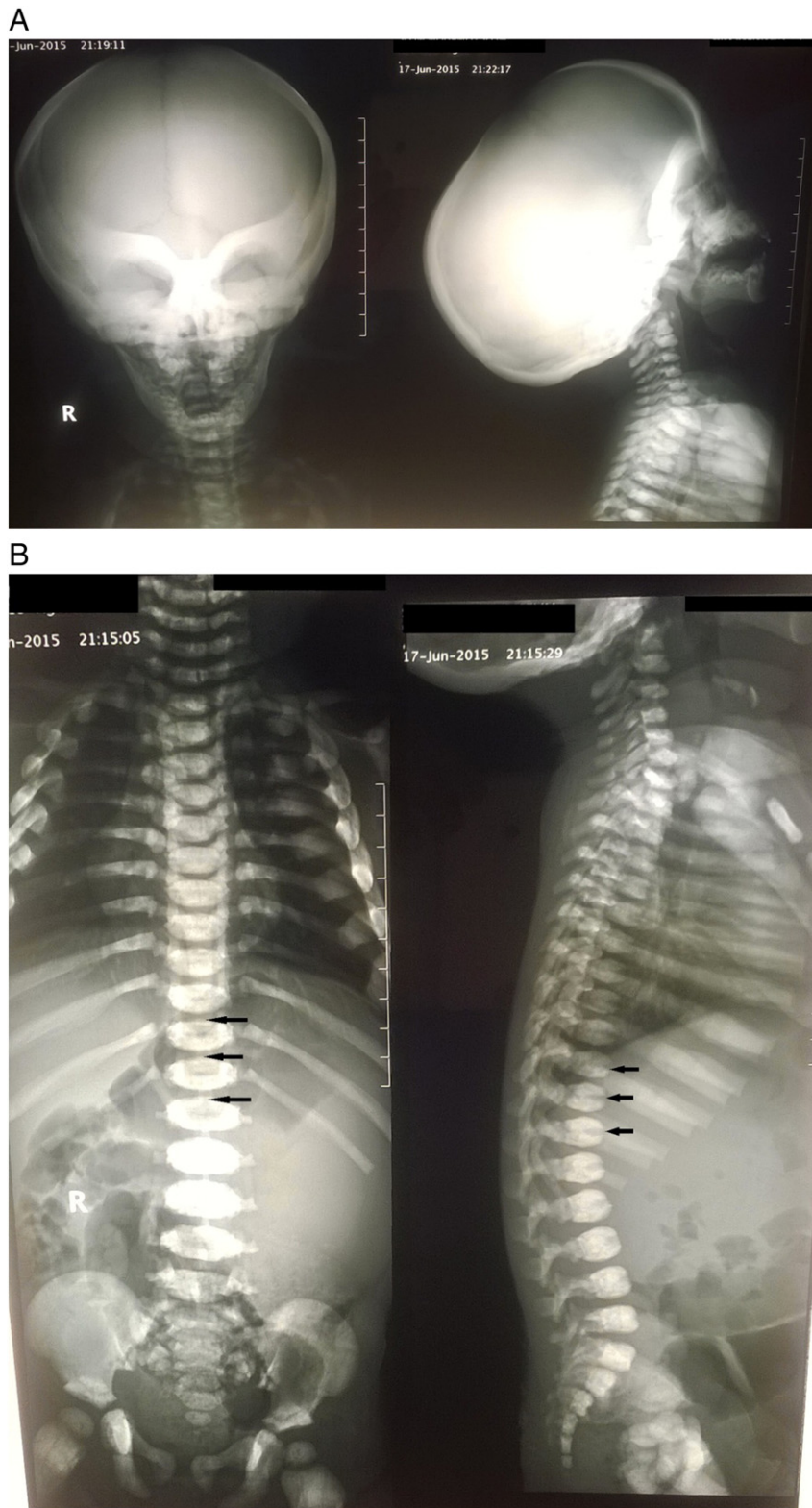


Fig. 1. Anteroposterior and lateral radiographs of the skull (A) and the spine (B) demonstrating an overall increased density of the bones with fundamental involvement of the medullary portion. Note the classic endobone or “bone-within-bone” appearance in the spine, the “sandwich vertebra” appearance, characterized by dense endplate sclerosis with sharp margins (black arrows).

Radiographic examination of the axial and appendicular skeleton revealed generalized osteosclerosis within the medullary portion of the bone with relative sparing of the cortices. Detailed radiographic abnormalities are depicted in Figs. 1A, B and 2A, B, C, D. The pelvi-abdominal sonography revealed splenomegaly with

no focal lesions. The blood picture revealed moderate anaemia. Our patient's parents were informed that data concerning the case would be submitted for publication. The authors report no conflict of interest concerning the materials or methods used in this study or the findings specified in this paper. No financing was received

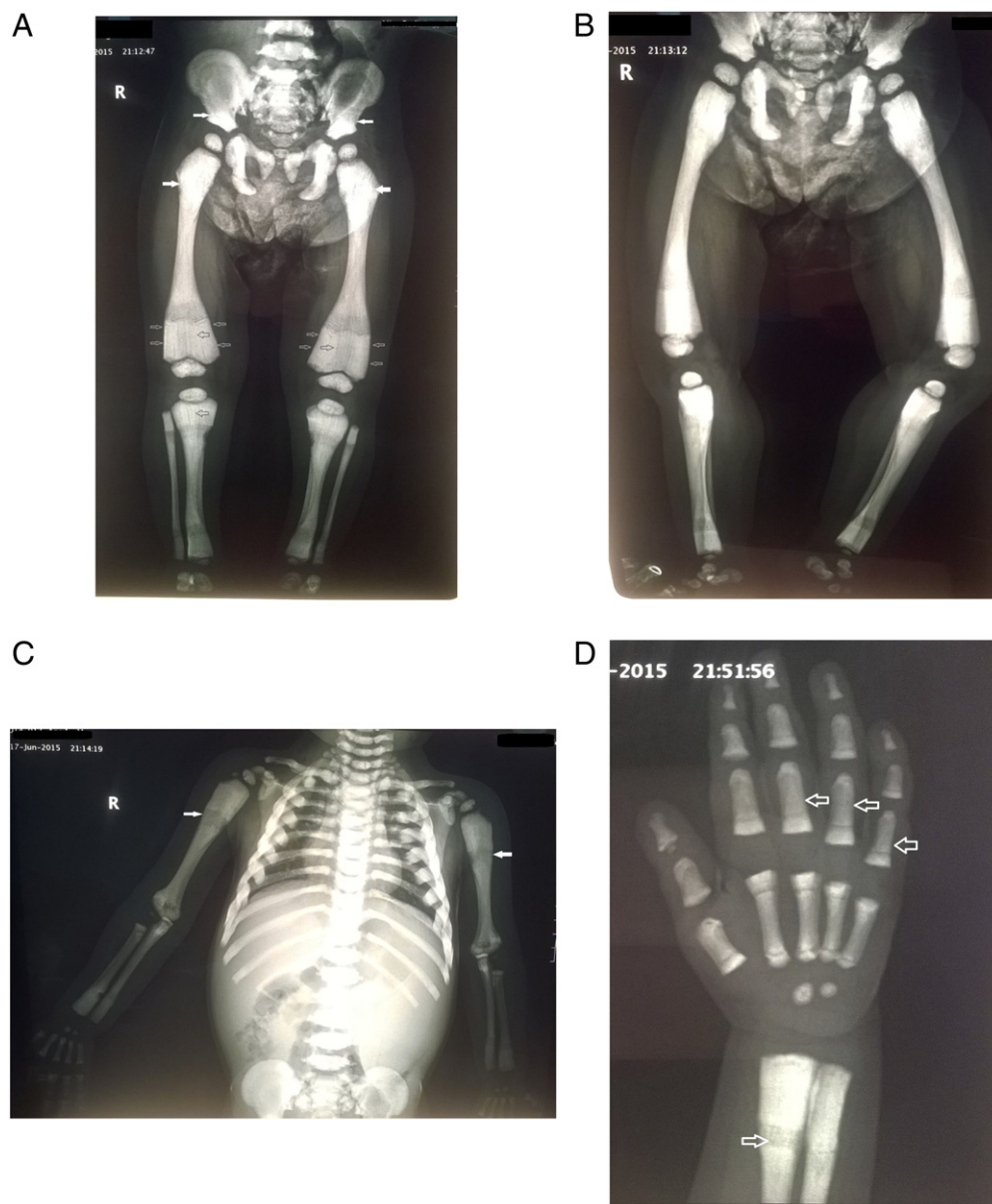


Fig. 2. Radiographs showing antero-posterior (A) and lateral views (B) of the pelvis and both lower limbs. Antero-posterior view of the chest wall and both upper limbs (C) and left hand (D). Note the uniform sclerosis of the pelvis and long bones of the lower limbs (A, B) long bones of the upper limbs (C) and short tubular bones (D). The classic “bone-within-bone” appearance is recognizable in the pelvis and proximal femora (white arrows) (A) and upper limbs (white arrows) (C) and short tubular bones of the hand (hollow arrows) (D). Note the Erlenmeyer flask deformity type 2 which is characterized by absence of normal diaphyseal metaphyseal modelling of the distal femora with abnormal radiographic appearance of trabecular bone (hollow white arrows) and alternating radiolucent metaphyseal bands (hollow black arrows) (A).

for this study. The study was authorized by the local ethical committee.

3. Discussion

The principals of clinical assessment of skeletal dysplasias include accurate history regarding time of onset of short stature prior to physical examination. Some dysplasias have prenatal onset, while others may only present either as newborns or beyond 2 to 3 years of age. Nonetheless some generalized bone mineralization abnormalities such as osteogenesis imperfecta, some osteosclerotic disorders as osteopetrosis, and hypophosphatasia may present with near normal proportions (Krakow and Rimoin, 2010). Our patient presented with near normal stature and proportions, but other associated symptoms and radiologic findings presented in infancy. These findings go in line with those reported by the previous authors.

Osteopetrosis is considered to be the prototype of sclerosing dysplasia, it is characterized by wide clinical and genetic heterogeneity with a common end-pathway of failure of normal osteoclastic resorption of bone and increased density in medullary portions of bones with sparing of cortices. The diagnosis also relies greatly on radiographic appearance of the skeleton (Ihde et al., 2011; Vanhoenacker et al., 2000).

Panda and colleagues described in their recent review article, a radiographic approach and review of common non-lethal skeletal dysplasias (Panda et al., 2014). They reported the essential radiological features of IO. These include; diffuse sclerosis involving both the skull vault, multiple limb fractures despite increased density, metaphyseal flaring leading to (Erlenmeyer flask deformity), and “Bone-within-bone” appearance typically noted in spine, pelvis and short tubular bones. In spine, this is termed as a sandwich vertebrae appearance due to end-plate sclerosis and relative lucency of center of body. In the pelvis, they appear as multiple dense white lines parallel to the iliac crest.

Table 1

Differential diagnosis of hereditary sclerosing bone dysplasias in children and adolescents (Stark and Savarirayan, 2009; Ihde et al., 2011; Maranda et al., 2008; Steward, 2003; Jacquemin et al., 1998; Whyte, 1993; Guerrini et al., 2008; Kilic and Etzioni, 2009; Benichou et al., 2000).

Dysplasia	Pathogenetics	Onset/prognosis	Skeletal radiology	Clinical findings
Infantile ("classic") osteopetrosis (IO)	Target site: endochondral ossification (primary spongiosa). Inheritance: AR. Genetic defect: <i>TCIRG1</i> with a localized defect located on chromosome 11q13. <i>SNX10</i> mutation was recently shown in 4% only of IO. There is defective osteoclast function and overgrowth of bone: which becomes thick dense and sclerotic, resulting in weak and brittle bones. Hypocalcemia may occur	Perinatal/poor. Fatal in infancy. HSCT is a treatment option	Generalized osteosclerosis of the axial and appendicular skeleton within the medullary portion of the bone with relative sparing of the cortices. Bone within a bone appearance, Sandwich vertebrae, failure of modelling of distal femora (Erlenmeyer flask deformity), alternating radiolucent metaphyseal bands. Pathological fractures and osteomyelitis	Pancytopenia, failure to thrive, cranial nerve deficits (II, VII, VIII), impaired vision, hepatosplenomegaly, obstructive hydrocephalus, poor dentition, and hypocalcemic seizures. Patients with <i>SNX10</i> have less severe clinical picture
Neuropathic IO	Inheritance: AR. Genetic defect: <i>CLCN7</i> , <i>OSTM1</i> . It is due to primary neurodegeneration not dissimilar to neuronal ceroid-lipofuscinosis, a lysosomal storage disorder. Electron microscopy of skin biopsies reveals swollen unmyelinated axons that contain spheroids, reduced numbers of myelinated axons and the presence of secondary lipofuscin-containing lysosomes in Schwann cells	Perinatal/poor. Fatal in infancy (extremely rare)	A homogenous and diffuse increase of density, consistent with osteopetrosis. Bone densitometry of lumbar spine showed a BMD at + 10SD above the mean for age.	Seizures in the setting of normal calcium levels, developmental delay, hypotonia, retinal atrophy with absent evoked visual potentials and sensorineural deafness
IO with renal tubular acidosis (RTA)	Inheritance: AR. Carbonic anhydrase (CA) isoenzyme II deficiency	Infancy or early childhood/variable. May benefit from HSCT	Classical radiographic features of osteopetrosis are present	Milder course where RTA and cerebral calcifications are typical. Other clinical manifestations comprise an increased frequency of fractures, short stature, dental abnormalities, cranial nerve compression, mental and developmental delay
IO with immunodeficiency (OLEDAID)	Inheritance: X-linked. Genetic defect: <i>IKBKG</i> (<i>NEMO</i>). AR subtype due to osteoclast-poor IO has been recognized as due to a defect in <i>TNFSF11</i> (<i>RANKL</i>). Bone biopsy reveals few/no osteoclasts	Infancy/poor. Fatal in early childhood.	Classical radiographic features of osteopetrosis are present.	Osteopetrosis, lymphedema, anhidrotic ectodermal dysplasia and immunodeficiency (OLEDAID). In AR subtype visual impairment, neurodevelopmental delay, hypocalcemic seizures, and recurrent infections may occur due to hypogammaglobulinemia
IO with leukocyte adhesion deficiency syndrome (LAD-III)	Inheritance: AR. Genetic defect: mutation in the <i>CalDAG GEF1</i> , <i>Kindlin-3</i>	Infancy/Poor. (extremely rare)	Classical radiographic features of osteopetrosis are present.	Recurrent infections accompanied by severe bleeding episodes and neurodevelopmental defects.
Intermediate osteopetrosis (IRO)	Inheritance: AR. Genetic defect: <i>CLCN7</i> , <i>PLEKHM1</i>	Childhood/Variable	Classical radiographic features of osteopetrosis are present.	Anaemia, extramedullary haematopoiesis, occasional optic nerve compression, pathological fractures, osteomyelitis and dental abnormalities.
Autosomal dominant osteopetrosis (ADO) (Albers-Schonberg)	Inheritance: AD. Genetic defect: <i>CLCN7</i> Less data than in IO are available on the cellular mechanism of decreased bone resorption in ADO but there is also genetic heterogeneity in ADO	Late childhood or adolescence/normal life expectancy	The classic bone-within-bone appearance was present in most but not all skeletal sites. Radiological penetrance of the disease increased after 20 years of age.	Main complications are confined to the skeleton, including fractures with delayed union, scoliosis, hip osteoarthritis and osteomyelitis, especially the mandible in association with dental abscess or caries. Cranial nerve compression is a rare, with hearing and visual loss affecting around 5% of individuals.
Pyknodysostosis (osteopetrosis acro-osteolytica)	Target site: endochondral ossification (secondary spongiosa). Inheritance: AR. Genetic defect: <i>CTSK</i> . Lysosomal disorder due to genetic deficiency in Cathepsin K which has been mapped to chromosome 1q21. Cathepsin K is essential for normal osteoclast function	Infancy or early childhood	Generalized osteosclerosis but with relative sparing of the medullary canal of long bones. Partial/total aplasia of terminal phalanges of the hand with sclerosis simulating acro-osteolysis which is considered an essentially pathognomonic feature. Marked delay in cranial suture closure and clavicle hypoplasia. In the spine characteristic sparing of the transverse processes	Disproportionate dwarfism, pathologic long bone fractures
Osteopoikilosis (Buschke-Ollendorff syndrome)	Target site: endochondral ossification (secondary spongiosa). Inheritance pattern: AD. Genetic defect: <i>LEMD3</i> . Patches of dense cortical like bone complete with haversian canals located within the spongiosa, often just deep to the cortex mainly in the inner cortex	Childhood or adulthood (rare)	Osteosclerotic foci that occur in the epiphyses and metaphyses of long bones, wrist, foot, ankle, pelvis, and scapula. Foci are either connected to adjacent trabeculae of spongy bone or attached to the subchondral cortex "enostosis"	Asymptomatic and incidentally found on radiographs. Bone strength is normal. It may manifest by multiple non tender subcutaneous nevi or nodules. Some individuals have both skin and bone manifestations, whereas others may lack skin or bone manifestations. Cooccurrence of osteopoikilosis and melorheostosis has been observed

Table 1 (continued)

Dysplasia	Pathogenetics	Onset/prognosis	Skeletal radiology	Clinical findings
Osteopathia striata with cranial sclerosis	Target site: endochondral ossification (secondary spongiosa). Inheritance pattern: X-linked dominant. Genetic defect: <i>AMER1</i> . Unknown pathology. Variants: Osteopathia striata without cranial sclerosis	Childhood/incidental in adulthood. (rare)	Sclerosis of the long bones and skull, and longitudinal striations visible on radiographs of the long bones, pelvis, and scapulae	Presents in females with macrocephaly, cleft palate, mild learning disabilities. In males, the disorder is usually associated with foetal or neonatal lethality. Osteopathia striata without cranial sclerosis is typically asymptomatic, although there can be associated joint discomfort
Mixed sclerosing bone dysplasia	A very rare disorder characterized by a variable combination of melorheostosis, osteopoikilosis and osteopathia striata. The disease may be generalized or may show unilateral involvement			
Progressive diaphyseal dysplasia (Camurati–Engelmann)	Target site: intramembranous ossification. Inheritance pattern: AD. Genetic defect: <i>TGFB1</i> , <i>R218C</i> . It is due to osteoblastic overactivity. Alkaline phosphatase levels are commonly elevated	Childhood (rare)	Tends to be bilateral and symmetrical. Can affect any bone but there is a special predilection to the long bones. Osteosclerosis occurs along the periosteal and endosteal surfaces of long bones. The epiphyses are spared	Waddling gait, musculoskeletal aches, weakness. Patients can have hepatosplenomegaly and compressive optic neuropathy
SOST-related sclerosing bone dysplasias	Target site: intramembranous ossification. Van Buchem disease (VBD); inheritance: AR. Genetic defect: A deletion affecting the <i>SOST</i> gene alters expression of sclerostin in osteoblasts causing failure of osteoblastic bone formation. Sclerosteosis; inheritance: AR, AD. Genetic defect: two independent mutations in <i>SOST</i> . Worth disease; inheritance pattern: AD	Childhood (extremely rare)	Diffuse endosteal sclerosis osteosclerosis and hyperostosis of the skeleton, prominently observed in cranial and tubular bones	VBD: facial distortions, cranial nerve affection. Sclerosteosis: progressive skeletal overgrowth. Syndactyly is a variable manifestation. Worth disease: facial abnormalities, no facial nerve involvement, osseous prominence of the palate

Note: AR: Autosomal recessive, AD: Autosomal dominant, HSCT: Haematopoietic Stem Cell Transplantation.

There is a clear agreement between the radiographic findings reported in the previous study and those reported in our case. Nonetheless our patient lacked any pathologic fractures. The use of internal fixation in treatment of pathologic fractures in osteopetrosis has been reported in adults (Aslan et al., 2014; Benichou et al., 2000).

Erlenmeyer flask bone deformity (EFD) is a long-standing term used to describe a specific abnormality of the distal femora. The deformity consists of lack of modelling of the diaphysis and metaphysis with abnormal cortical thinning and lack of the concave diaphyseal metaphyseal curve. Utilizing a literature review and cohort study of 12 skeletal dysplasias, Faden and colleagues classified EFD into three groups and determined which skeletal dysplasias or syndromes were highly associated with that specific deformity (Faden et al., 2009). They associated IO with the second group characterized by absence of normal diaphyseal metaphyseal modelling with abnormal radiographic appearance of trabecular bone. The description of the distal femoral deformities in IO offered by the previous authors is in accordance with radiographic findings demonstrated in our case.

Ihde and colleagues conducted an excellent review article on sclerosing bone dysplasias and their differential diagnosis (Ihde et al., 2011). The radiographic findings of IO reported by the previous study was similar to those described in our case. Table 1 provides a summary of the differential diagnosis of hereditary sclerosing bone dysplasias presenting in childhood, in regards to pathogenetics and radioclinical features.

3.1. Genetic profiling

Nearly half of cases infantile autosomal recessive osteopetrosis involve mutation of *TCIRG1* gene. This is followed by mutations of *CLCN7* which is responsible for 13% of cases. The clinical picture of both is similar but patients with *CLCN7* mutations have more developmental delay and convulsions (Frattini et al., 2003). Nearly 4% of cases of autosomal recessive osteopetrosis involves mutations in *SNX10* gene. Although the clinical picture seems to be milder, loss of vision, anaemia and

bone fragility is more common (Aker et al., 2012). *OSTM1* gene causes a very severe form of the disease with frequent CNS manifestations, the mutation of which is responsible for 2% of cases of infantile autosomal recessive osteopetrosis (Pangrazio et al., 2006). A very mild phenotype that can regress with age is caused by mutation of *PLEKHM1* gene (Van Wesenbeeck et al., 2007).

All these genes are involved in the acid secretion mechanism of osteoclasts, the mechanism by which osteoclasts causes bone resorption through its “extracellular lysosomes” (Teitelbaum and Ross, 2003). For example, the *CLCN7* gene encodes the chloride channel that resides in lysosomal vesicles and is thought to transport negative charge in parallel to the proton pumped into the resorption lacunae by the membrane H-ATPase. *TCIRG1* gene encodes an important subunit of this H-ATPase (Kornak et al., 2001). Molecular diagnosis was not conducted in our patient. Nevertheless we suggest that testing of *TCIRG1* gene at first is appropriate, because of the mild developmental delay and absence of other manifestations as; convulsions, and loss of vision.

4. Conclusion

Although tremendous advances have been made in the elucidation of the genetic defect of osteopetrosis over the past years, the role of accurate clinical and radiological assessment remains an important contributor to the diagnosis of infantile osteopetrosis.

References

- Aker M, Rouvinski A, Hashavia S, Ta-Shma A, Shaag A, Zenvirt S, et al. An *SNX10* mutation causes malignant osteopetrosis of infancy. *J. Med. Genet.* 2012;49:221–6. <http://dx.doi.org/10.1136/jmedgenet-2011-100520>.
- Aslan, A., Baykal, Y.B., Uysal, E., Atay, T., Kirdemir, V., Baydar, M.L., et al., 2014. Surgical treatment of osteopetrosis-related femoral fractures: two case reports and literature review. *Case Rep. Orthop.* 2014, 891963. <http://dx.doi.org/10.1155/2014/891963>.
- Benichou, O.D., Laredo, J.D., de Vernejoul, M.C., 2000. Type II autosomal dominant osteopetrosis (Albers-Schonberg disease): clinical and radiological manifestations in 42 patients. *Bone* 26, 87–93. [http://dx.doi.org/10.1016/S8756-3282\(99\)00244-6](http://dx.doi.org/10.1016/S8756-3282(99)00244-6).
- Faden, M.A., Krakow, D., Ezgu, F., Rimoin, D.L., Lachman, R.S., 2009. The Erlenmeyer flask bone deformity in the skeletal dysplasias. *Am. J. Med. Genet. A* 149A, 1334–1345. <http://dx.doi.org/10.1002/ajmg.a.32253>.

- Frattini A, Pangrazio A, Susani L, Sobacchi C, Mirolo M, Abinun M, et al. Chloride channel CICN7 mutations are responsible for severe recessive, dominant, and intermediate osteopetrosis. *J. Bone Miner. Res.* 2003;18:1740–7. <http://dx.doi.org/10.1359/jbmr.2003.18.10.1740>
- Guerrini, M.M., Sobacchi, C., Cassani, B., Abinun, M., Kilic, S.S., Pangrazio, A., et al., 2008. Human osteoclast-poor osteopetrosis with hypogammaglobulinemia due to TNFRSF11A (RANK) mutations. *Am. J. Hum. Genet.* 83, 64–76. <http://dx.doi.org/10.1016/j.ajhg.2008.06.015>.
- Ihde, L.L., Forrester, D.M., Gottsegen, C.J., Masih, S., Patel, D.B., Vachon, L.A., et al., 2011. Sclerosing bone dysplasias: review and differentiation from other causes of osteosclerosis. *Radiographics* 31, 1865–1882. <http://dx.doi.org/10.1148/rg.317115093>.
- Jacquemin, C., Mullaney, P., Svedberg, E., 1998. Marble brain syndrome: osteopetrosis, renal acidosis and calcification of the brain. *Neuroradiology* 40, 662–663. <http://dx.doi.org/10.1007/s002340050660>.
- Kilic, S.S., Etzioni, A., 2009. The clinical spectrum of leukocyte adhesion deficiency (LAD) III due to defective CalDAG-GEF1. *J. Clin. Immunol.* 29, 117–122. <http://dx.doi.org/10.1007/s10875-008-9226-z>.
- Kornak U, Kasper D, Bosl MR, Kaiser E, Schweizer M, Schulz A, et al. Loss of the CIC-7 chloride channel leads to osteopetrosis in mice and man. *Cell.* 2001;104:205–15. [http://dx.doi.org/10.1016/S0092-8674\(01\)00206-9](http://dx.doi.org/10.1016/S0092-8674(01)00206-9)
- Krakow, D., Rimoin, D.L., 2010. The skeletal dysplasias. *Genet. Med.* 12, 327–341. <http://dx.doi.org/10.1097/GIM.0b013e3181daae9b>.
- Maranda, B., Chabot, G., Decarie, J.C., Pata, M., Azeddine, B., Moreau, A., et al., 2008. Clinical and cellular manifestations of OSTM1-related infantile osteopetrosis. *J. Bone Miner. Res.* 23, 296–300. <http://dx.doi.org/10.1359/jbmr.071015>.
- Panda, A., Gamanagatti, S., Jana, M., Gupta, A.K., 2014. Skeletal dysplasias: a radiographic approach and review of common non-lethal skeletal dysplasias. *World J. Radiol.* 6 (10), 808–825. <http://dx.doi.org/10.4329/wjr.v6.i10.808>.
- Pangrazio A, Poliani PL, Megarbane A, Lefranc G, Lanino E, Di Rocco M, et al. Mutations in OSTM1 (grey lethal) define a particularly severe form of autosomal recessive osteopetrosis with neural involvement. *J. Bone Miner. Res.* 2006;21:1098–105. <http://dx.doi.org/10.1359/jbmr.060403>
- Sit, C., Agrawal, K., Fogelman, I., Gnanasegaran, G., 2015. Osteopetrosis: radiological & radionuclide imaging. *Indian J. Nucl. Med.* 30 (1), 55–58. <http://dx.doi.org/10.4103/0972-3919.147544>.
- Stark, Z., Savarirayan, R., 2009. Osteopetrosis. *Orphanet J. Rare Dis.* 4, 5. <http://dx.doi.org/10.1186/1750-1172-4-5>.
- Steward, C.G., 2003. Neurological aspects of osteopetrosis. *Neuropathol. Appl. Neurobiol.* 29, 87–97. <http://dx.doi.org/10.1046/j.1365-2990.2003.00474.x>.
- Teitelbaum SL, Ross FP. Genetic regulation of osteoclast development and function. *Nat. Rev. Genet.* 2003;4:638–49. <http://dx.doi.org/10.1038/nrg1122>.
- Van Wesenbeeck L, Odgren PR, Coxon FP, Frattini A, Moens P, Perdu B, et al. Involvement of PLEKHM1 in osteoclastic vesicular transport and osteopetrosis in incisors absent rats and humans. *J. Clin. Invest.* 2007;117:919–30. <http://dx.doi.org/10.1172/JCI30328>.
- Vanhoeacker, F.M., De Beuckeleer, L.H., Van Hul, W., Balemans, W., Tan, G.J., Hill, S.C., et al., 2000. Sclerosing bone dysplasias: genetic and radioclinical features. *Eur. Radiol.* 10 (9), 1423–1433 (PMID: 10997431).
- Whyte, M.P., 1993. Carbonic anhydrase II deficiency. *Clin. Orthop. Relat. Res.* 294, 52–63 (PMID: 8358947).